



Failure Analysis of Unconfined Brick Masonry with Experimental Verification

Anjani Kumar Shukla · Saurav Kumar · P. R. Maiti

Submitted: 4 October 2020 / in revised form: 23 December 2020 / Accepted: 11 January 2021 / Published online: 2 February 2021
© ASM International 2021

Abstract The survival of low rise unconfined masonry structure against earthquakes is very rare even due to low or moderate intensity events. To understand the failure mechanism and cracking pattern of unconfined masonry, a scaled specimen of four unconfined brick was analyzed using finite element software in conjunction with experimental verification. This study started by developing 3D finite element model of unconfined masonry subjected to in-plane loading. Bricks and joints were modeled discretely in the model, allowing for nonlinear deformation characteristics of the both materials. This model exhibits the local effect and is capable of displaying the behavior of masonry walls in which high local stresses and stress gradients are presented in the color contour diagram. The overall result of stress is presented using the von Mises (distortion energy method). The analysis of the model concluded that the unconfined brick masonry specimen structure generally fails along the brick joints, although in-plane shear stresses can cause cracks through the brick in the translation to tensile stress zone.

Keywords Finite element analysis · Masonry structure · Earthquake resistant structure · ANSYS modeling · Unconfined brick masonry

Introduction

The major portion of masonry construction around the world is unconfined. During earthquakes, these structures have shown very poor performance, resulting in cracking and sometimes collapse. Masonry always performed extremely well in the compression, so the other two stress zones tension and shear consistently become a matter of investigation. Tension and shear depend greatly on the two factors; first is the quality of mortar and second is the loading configuration on the masonry [1]. The construction method of unconfined brick masonry is very ancient and conventional, and there was less provision for modern requirement of earthquake-resistant structures as no such codal provision available so that these buildings performed poorly at the time of the earthquake [2]. According to the research, the most common modes of failure of unconfined masonry buildings are of two types: a) Crushing of concrete at the joints between vertical tie columns and horizontal bond beams and b) failure of mortar upper layer between brick and mortar which can cause the failure at the time of earthquake [3]. Horizontal cracks at the joints between masonry walls, reinforced concrete floors and at foundation can be observed if the lateral movement of the earth may take place [4]. Shear cracks in masonry panels that propagate into the tie columns can cause sudden collapse at the time of earth-shaking. Else it can be a cause of column failure followed by complete collapse can occur [5]. Mortar laced in the vertical direction control the deformation of masonry structure especially nonlinear characteristics. Generally, failure of vertical concrete leads to the failure of masonry like if cracks appear in window piers and walls due to in-plane and out-of-plane action in inadequate confinement of walls, it could be a dangerous sign and lead

A. K. Shukla (✉) · P. R. Maiti
Department of Civil Engineering, Indian Institute of Technology
(BHU), Varanasi, India
e-mail: akshukla.rs.civ16@iitbhu.ac.in;
er.anjanishukla@gmail.com

S. Kumar
Department of Civil Engineering, JAYPEE University, Solan,
H.P., India

to failure of masonry structure [6]. The present study covers finite element modeling and failure analysis of brick masonry, stress analysis of brick masonry using ANSYS and analysis of different stresses in brick masonry wall for different boundary conditions. Generally, masonry prisms show nonlinearity, so an accurate method is necessary for simulations. The convergence criterion was set at 10^{-6} because the relatively small value will minimize the computation error and will not allow it to exceed the simulation errors [7]. The unreinforced masonry has least lateral load capacity, and it can improve by confining it. If the wall of unconfined masonry can be connected through reinforcement from wall to wall because the horizontal wall bars will generate good amount of lateral strength with axial load taking capacity and will develop ductility [8]. A U-shaped connecting reinforcement from wall to column or from wall to wall can prevent the separation of wall from column [9]. Increment in vertical axial stress resulting the increment in the lateral load capacity of brick wall, which can predict the flexural capacity of the wall [10].

Stress Distribution in Brick samples

The masonry structure especially made of bricks is two-phased material. Both the phases have different deformation pattern as well as different strengths. It is certain that the modulus of elasticity of cement mortar and compressive strength is sufficiently lower than that of bricks. It means if the cement will fail freely then its lateral cracks will be greater than that of bricks. The internal stress is developed between the mortar and bricks due to bond friction and confinement of cement so an internal stress is produced which includes lateral tension and axial compression in the bricks and triaxial compression in the mortar (Fig. 1).

Modeling of Masonry Prism

There are 100s of dissimilar element that can be found in the finite element software ANSYS in their library. Every element carries an individual number and a joint that recognize the category of an element, like **BEAM3**, **SOLID45**, **PLANE42**, etc. ANSYS divides the elements into 21 separate groups; in all that 21 types of element, our primary focus is on the structural group [11]. In this 3D modeling, SOLID45 is used for solid structures. Every element can be defined by eight nodes, and every node has three degrees of freedom: i.e., Translations in the nodal x, y, and z directions. The element has swelling, creep, plasticity, large deflection, stress stiffening, and large strain capacity. The node locations, geometry, and the coordinate system for this element are presented in Fig. 2 SOLID45

Geometry [12]. The element can be defined by orthotropic material properties also. The directions of orthotropic material can correlate to the coordinate element directions also. Pressures may be taken as surface loads on the element faces as presented by the circled numbers on geometry “SOLID45.” Positive pressures act as compressive force over the element.

Analytical Derivation for Axial Compressive Strength

Generally, mortar and brick joint surface go only into the biaxial stress state, it means it can be stated that the confinement of mortar is not adequate: Therefore, surface of brick may go into spalling condition at even lower stress which may cause progressive failure of structure. To describe the failure of brick under axial stress, Eq 1 is used:

$$\sigma_x = \sigma_z = f'_{bt} \left[1 - \frac{\sigma_y}{f'_b} \right] \quad (\text{Eq 1})$$

where $\sigma_x, \sigma_y, \sigma_z$ = stress in x, y, or z direction, f'_b = uniaxial compressive strength of bricks, f'_{bt} = strength of bricks under biaxial tension.

Minimum lateral tensile stress played role in the brick to efficiently confine the cement mortar. It rely on the development in the cement mortar under triaxial compression. Richard brandtzaag and brown (X) have studied about triaxial strength of concrete [13]. They concluded that triaxial strength of concrete can be expressed in Eq 2

$$f'_1 = f'_e + 4.1\sigma_2 \quad (\text{Eq 2})$$

where f'_1 = compressive strength of a laterally confined, f'_c = uniaxial compressive strength of concrete, σ_2 = lateral confinement.

Minimum lateral confinement of the mortar joint can be expressed as in Eq 3:

$$\sigma_{xj} = \frac{1}{4.1} (\sigma_y - f'_j) \quad (\text{Eq 3})$$

where σ_{xj} = lateral compressive stress in mortar joint, σ_y = local stress in Y direction, f'_j = uniaxial compressive strength of mortar.

Using the non-uniformity coefficient at failure U_u , the average stress in masonry at failure described in Eq 4

$$\sigma_{ym} = f'_m = \frac{\sigma_y}{U_u} \quad (\text{Eq 4})$$

So from here we can obtain equation for axial compressive strength of masonry as in Eq 5

$$f'_m = \frac{f'_b f'_{bt} + a f'_j}{U_u f'_{bt} + a f'_b} \quad (\text{Eq 5})$$

Fig. 1 Stress distribution in brick stack under concentric compression force

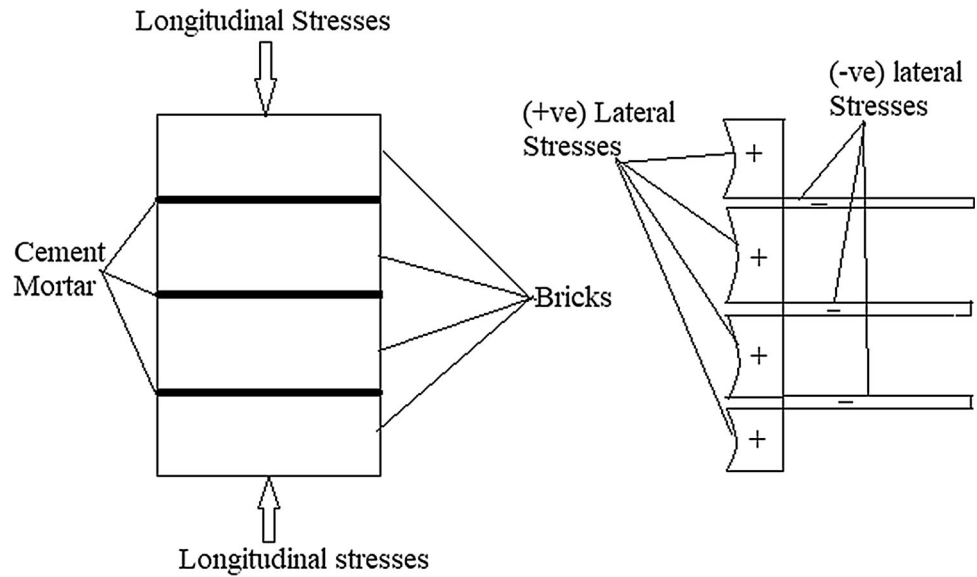


Fig. 2 Line diagram of Solid45 Element

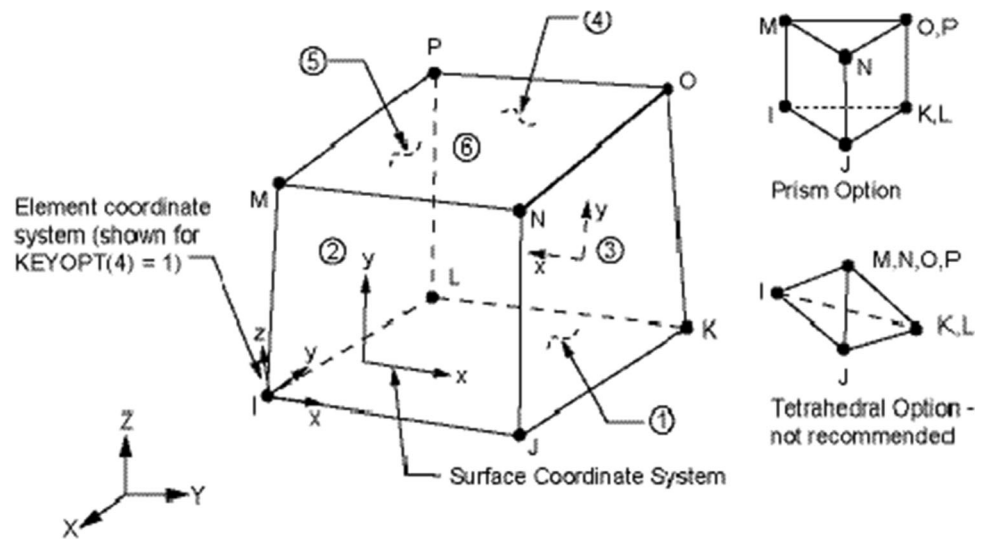


Table 1 Material properties of bricks

Properties	Value
(a) Bricks	
Elasticity modulus	14,700 MPa
Tensile strength	1.2 MPa
Poisson's ratio	0.16

Table 2 Mortar properties

Properties	Value
(a) Cement mortar	
Elasticity modulus	7400 MPa
Tensile strength	0.78 MPa
Poisson's ratio	0.21

Material Properties

The values of elasticity modulus (**EX**) and Poisson's ratio (**PRXY**) of first class brick have taken from Ali and page 1986 [14] to model the unconfined brick masonry in ANSYS and are tabulated in Tables 1 and 2.

Model Preparation on ANSYS

Details of Model (specimen M1)

Four numbers of rectangular brick blocks of standard size are used to model the unconfined brick masonry in

ANSYS, and mortar of thickness 10 mm is placed in between them as presented in Fig. 3.

Dimension of bricks : Length = 190 mm, Width = 90 mm Height = 90 mm

Model Detail of Specimen M2

A brick wall panel is modeled with rectangular bricks of standard size as mentioned above and mortar of 10 mm as a stretching bond as in Fig. 4, in which all bricks are laid as stretchers. The dimension of the wall is 1.99 m × 0.79 m × 0.09 m.

Meshing

To mesh this brick masonry volume 4–6 sided mapped meshing is used. The mapped meshing method is used only in the case of 2D and 3D problems (no line elements). The dimensions of solid model (volume and area) meshed with 4–6 side mapped meshing method option occupy quadrilateral area elements or hexahedral volume. The mapped meshed generates the regular block which is good for computational works. The mapped meshed volume is shown in Figs. 5 and 6 as follows.

Model Preparation in Laboratory

Material Specification

Bricks Locally available burnt clay bricks from a kiln are used in this experiment. Average size of the bricks was 22 cm × 10.5 cm × 6.5 cm. Water absorption test was performed to determine the water absorption of bricks. The average of 20 brick was found 13.5% which is acceptable for first class brick as per IS 1077-1973.

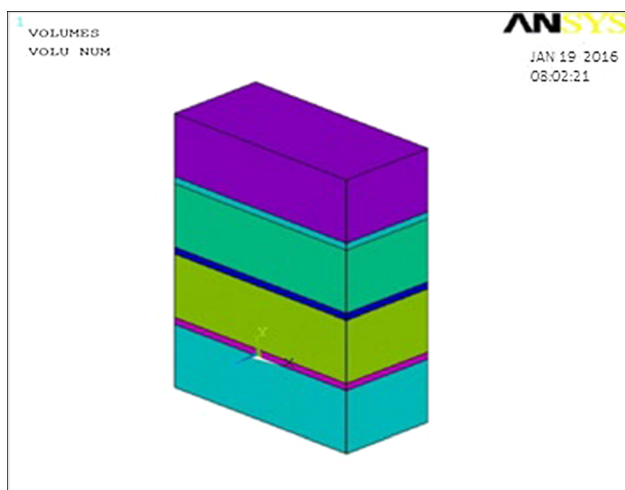


Fig. 3 Model prism M1

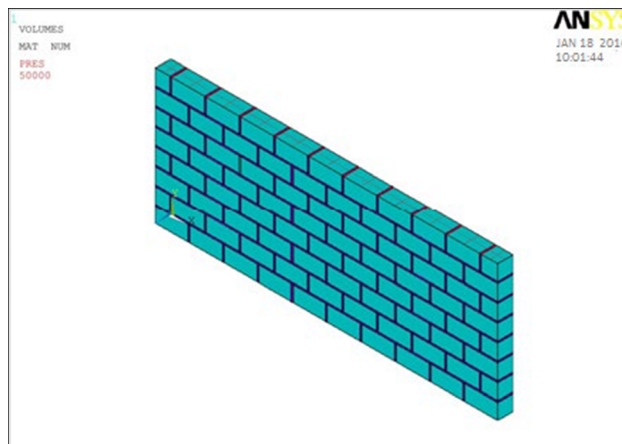


Fig. 4 Model of specimen M2

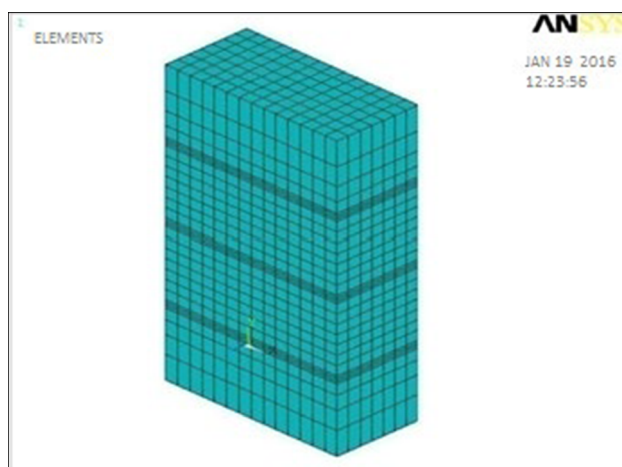


Fig. 5 Meshed model for specimen M1

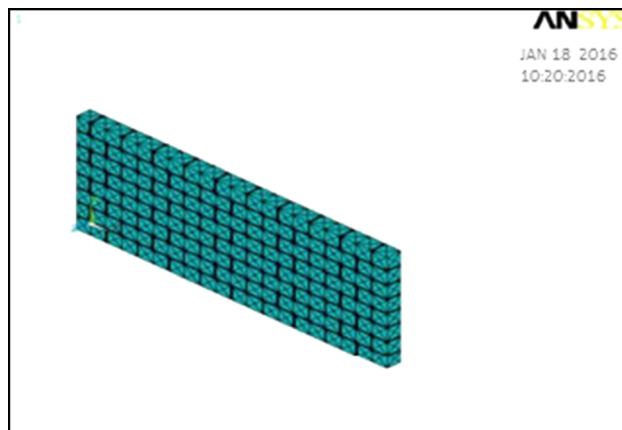


Fig. 6 Meshed model for specimen M2

Cement Portland Pozzolana cement PPC (Brand Name - Ultratech Cement), standard consistency test was performed and it was found out to 36%.

Sand Sand used in the preparation of mortar was natural sand.

Mortars Cement mortar; proportion: 1 cement/4 sand.

Casting and curing For Experimental verification, the four brick specimens were cast and cured for 28 days in tank. Refer Fig. 7 for casting and Fig. 8 for curing.

Results and Discussion

For analyzing the brick prism, different boundary condition was applied to explore all possible conditions of failure. In first case, one end of the prism (brick model) is fixed and the load is applied on the free end of the model. Uniform load of 70 kN, 80 kN, 90 kN was applied on the free end of the masonry. Along with the vertical load, a horizontal load of 10 kN was applied to the block to check the lateral strength of the prism. Different stress contours were collected, and with help of them, the different parameter's graph has been plotted.

Stress Calculation

Stress Calculation for Model M1 When Subjected to Vertical Load

The X component of stress is increasing parabolically from end to midway and is highest at the mean point (refer to



Fig. 8 Curing in laboratory

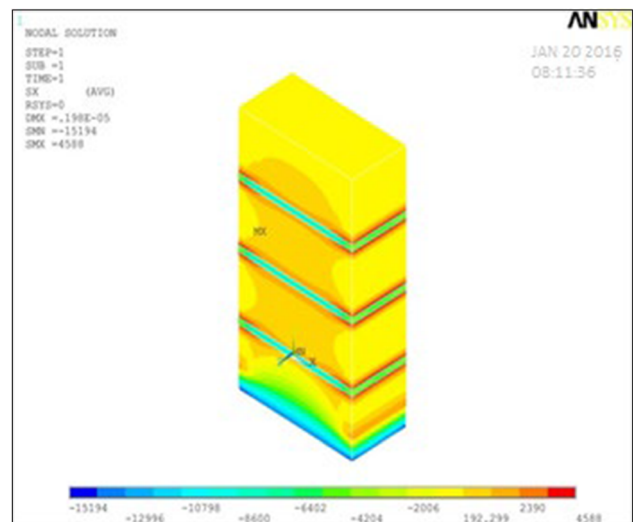


Fig. 9 X component stress

Fig. 9). Second and third bricks experience more stress than top and bottom courses. In Fig. 10, Y component of stress has more or less same values except at the lower points where it is more. And the joints of all bricks show higher stress with red marks. It means these locations are at high risk at the time of Y Loading.

Various Stress Computation for the Specimen with Experimental Verification

First principal stress: In Fig. 11, it can be observed that variation in 1st principal stress is similar to x component stress, but its values are lesser than that of x component of stress and the similar pattern can be verified by laboratory experiment in Fig. 12.

XY shear stress XY shear stress is more critical at the bottom corner of the masonry. Masonry prism tends to crack at the bottom first in compressive testing machine which can be verified in Fig. 13. The variation in XY shear stress along Y axis is shown in Fig. 14. Peak values are obtained at the place of brick mortar interface.



Fig. 7 View of the bricks with mortar

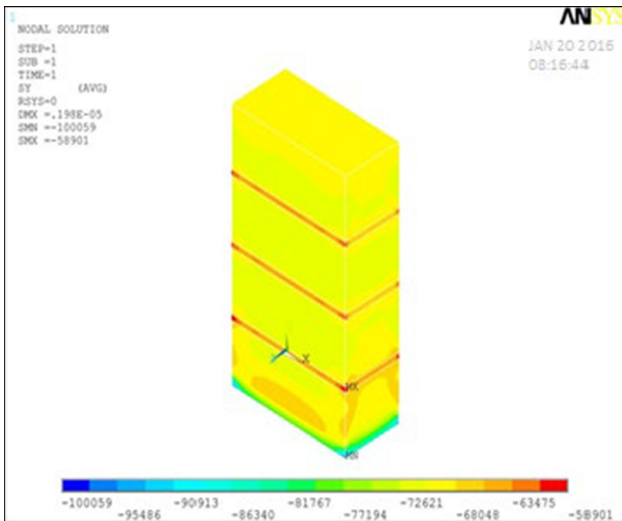


Fig. 10 Y component stress

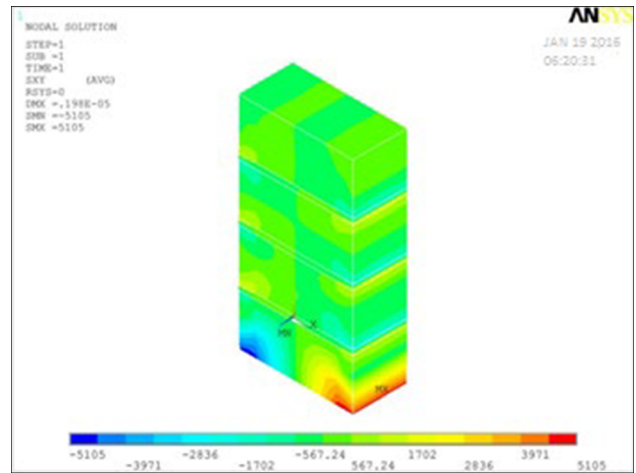


Fig. 13 XY shear stress

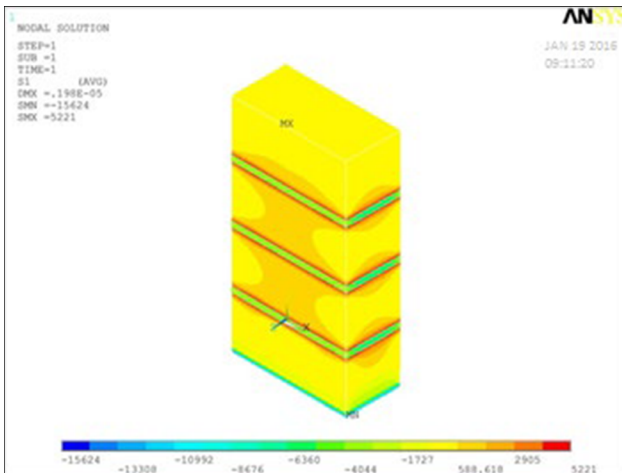
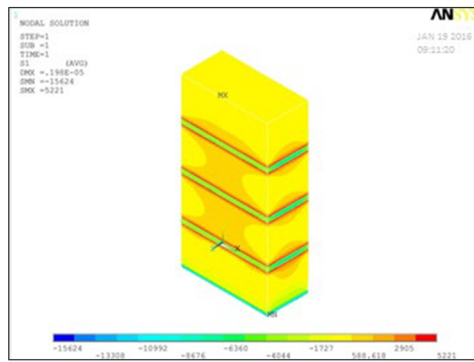


Fig. 11 First principal stresses

Fig. 12 Experimental verification



The variation in XY shear forces along Y axis is plotted in Fig. 15.

YZ shear stress When the force was applied on the YZ direction, the prism feels the force on its bottom face (Fig. 16). Variation in stress with distance along Y axis can be observed in Fig. 17.

XZ shear stress When the force was applied on the XZ direction, the stresses are imparted on joint corner of every brick (Fig. 18). Variation in stress with distance along Y axis can be observed in Fig. 19.

Von Mises stress The von Mises stress presented here which was obtained by finite element analysis of samples and the critical points has been displayed (Fig. 20) also the experimental verification of above sample can be seen in Fig. 21. Variation in stress with distance along Y axis can be observed in Fig. 22.



Fig. 14 Experimental verification of XY shear

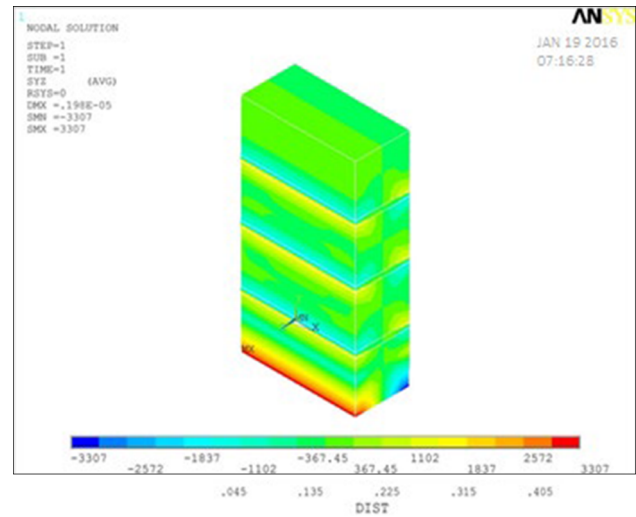


Fig. 16 YZ shear stress

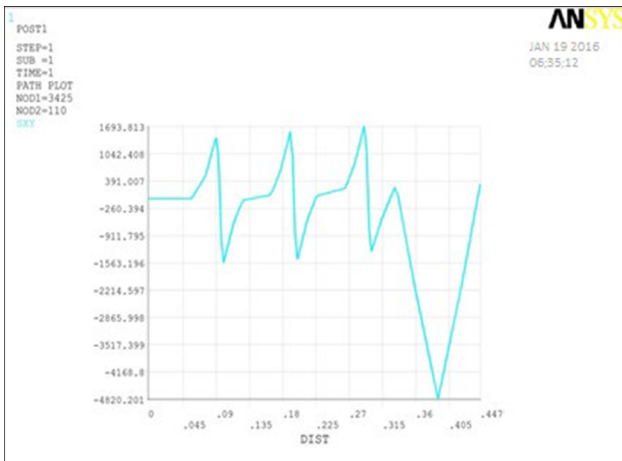


Fig. 15 Variation in XY shear stress along Y axis

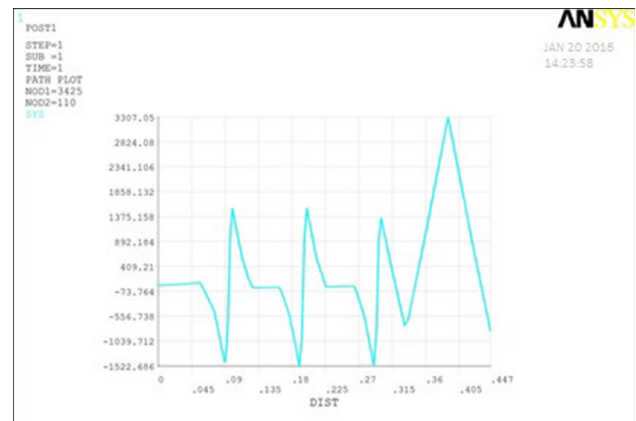


Fig. 17 Variation in YZ shear stress along Y axis

Figure 22 pointed that the shear stress increases with distance along Y axis. At a distance of 90 mm, stress is approximately 1400 Mpa but from 90 to 100 mm, i.e., at the level of mortar, it decreases abruptly to -1563 Mpa. Maximum shear stress measured 1693 Mpa at 28 mm.

Stress Calculation for Block M1 with Horizontal Loading and Vertical Loading

In this model, a vertical load of 70kn along with a horizontal load of 30kn was applied. Initially, the horizontal load was applied at the top brick. From Y component of stress, it can be seen that maximum stress occurs at the

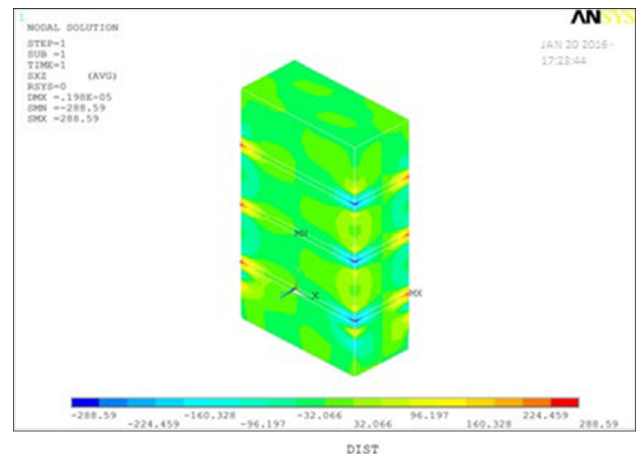


Fig. 18 XZ shear stress

bottom of the prism. Variation in von Mises stress can be observed from Figs. 23 and 24.

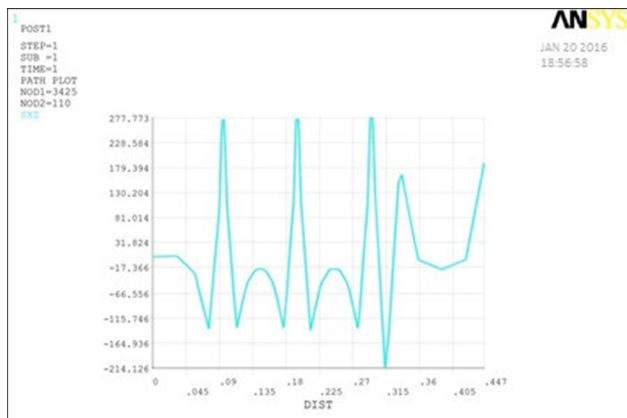


Fig. 19 Variation in XZ shear stress along Y axis

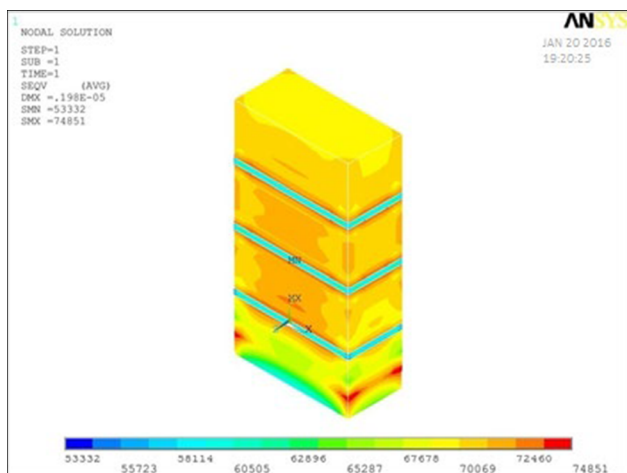


Fig. 20 Von Mises stress

Similarly, the stress in XY direction can be observed in Fig. 25 and verified which can be found in Fig. 26. And its von Mises stress verified the experimental output of stress in the laboratory (Fig. 27).

Again in this model, horizontal load is applied at the middle two bricks. It is observed from Fig. 28 that Y component of stress at the bottom most point has decreased. There is increased in von Mises stress when wind load is applied in the middle two bricks as shown in Fig. 29.

Stress Calculation for Block M2 with Horizontal and Vertical Loading

For specimen M2, simultaneously vertical and horizontal loading are applied to the wall, and its stress variations are observed. From Fig. 30, it is observed that due to application of horizontal loads, wall tends to deflect away in the direction of load. But another end of the wall has not



Fig. 21 Experimental verification of von Mises stress

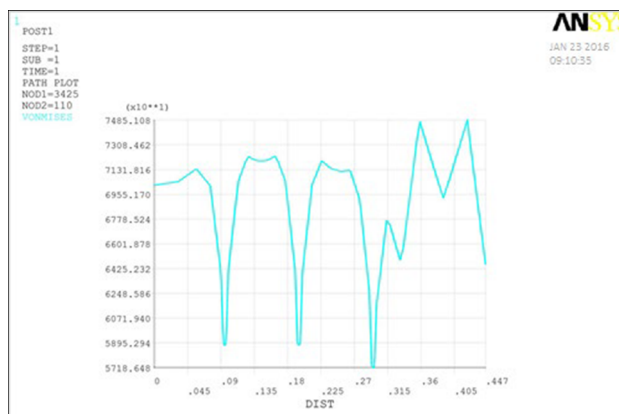


Fig. 22 Von Mises stress variation along Y axis

defected due to confinement. XY shear stress also decreases from top to bottom.

Conclusion

In the stress contours, red area is indicating the maximum stress at that particular point. After analyzing all stress contours, it can be concluded that at every boundary layer of brick–mortar joints of prism, maximum stress occurred and found the prism are prone to fail from these joints. Further, some more conclusions can be drawn here with the help of this study:

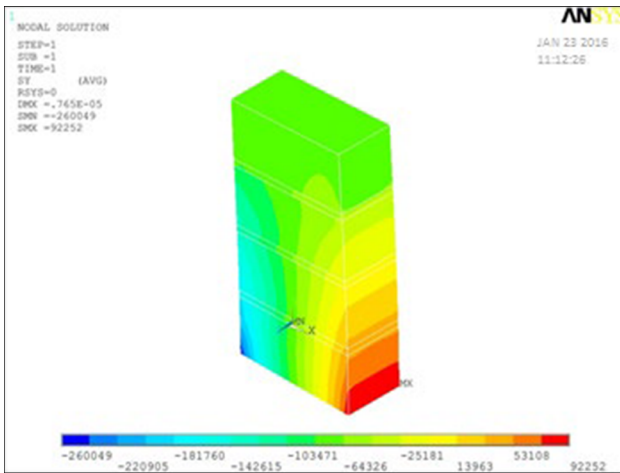


Fig. 23 Y component of stress



Fig. 26 Experimental verification



Fig. 24 Experimental verification

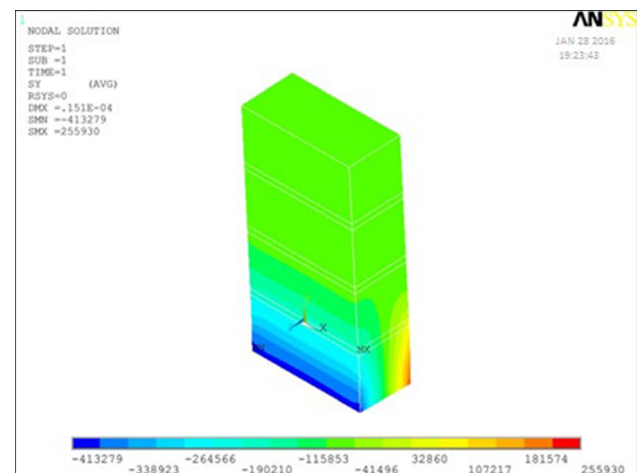


Fig. 27 Von Mises stress

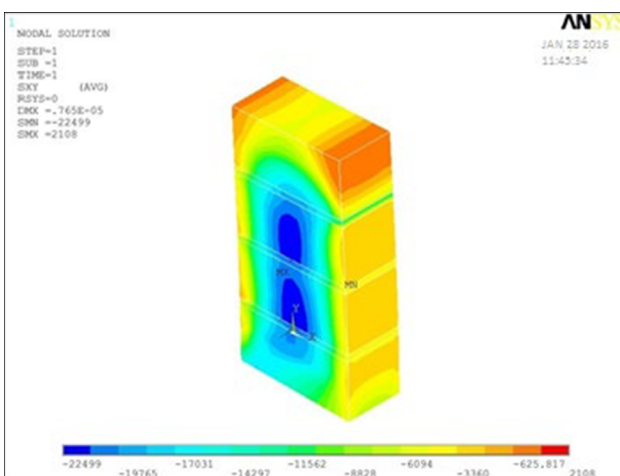


Fig. 25 XY shear stress

1. The normal unconfined brick masonry has very less strength toward the lateral forces. So it needs to be strengthened.
2. To increase the strength of masonry structure, strengthening of joints with adequate ductility is needed so that at the time of the earthquake, it can show some deflection before failure.
3. Wall to wall or wall to column reinforcement is must to confining the wall with the column or sidewall.
4. The stress was recorded maximum at the bottom and decreasing toward the midsection so the length of

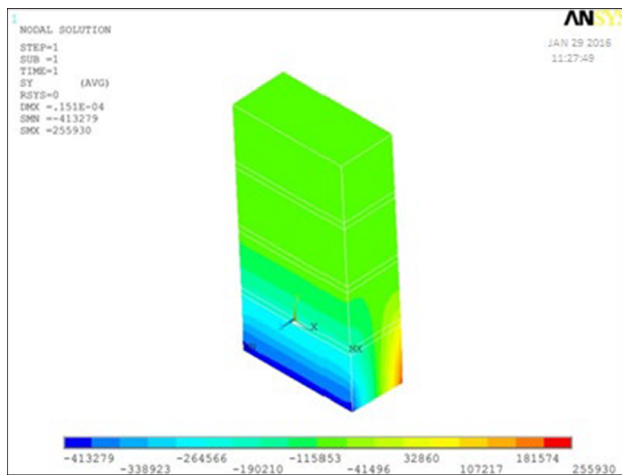


Fig. 28 Y component stress

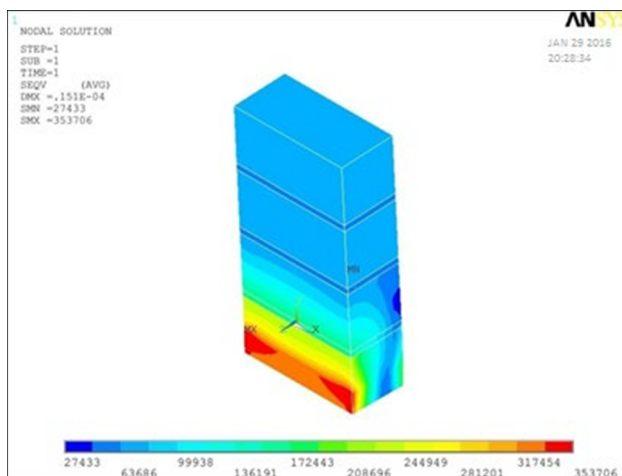


Fig. 29 Von Mises stress

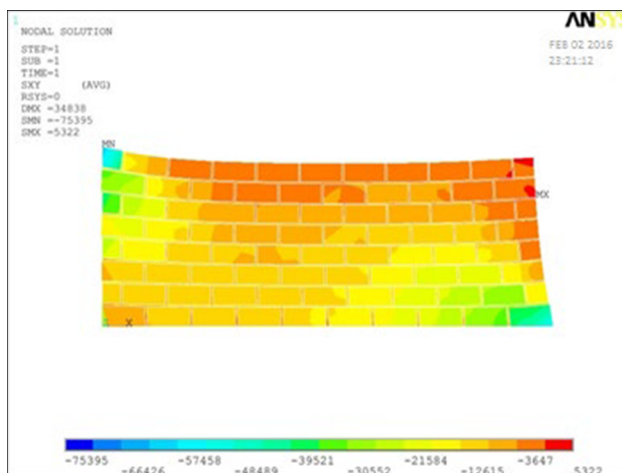


Fig. 30 XY shear stress

transverse reinforcement will be highest at bottom layer of brick–mortar and should be minimized toward the midsection. It will decrease the cost of confinement of the unreinforced masonry structure.

Further, scope of study in this area is to find the correct length of transverse bars, which will be used to tie the wall to wall or wall to column.

References

1. Yoshimura, K. et al. Experimental study for developing higher seismic performance of brick masonry walls, in *Proceedings of the 13th World Conference on Earthquake Engineering*, Vancouver, Canada, Paper No. 1597 (2004)
2. Blondet, M. Construction and Maintenance of Masonry Houses—For Masons and Craftsmen. Pontificia Universidad Catolica del Peru, Lima, Peru. <http://www.world-housing.net/> (2005)
3. S. Alcocer, J.G. Arias, L.E. Flores, *Some Developments on Performance-Based Seismic Design of Masonry Structures* (International Workshop on Performance-Based Seismic Design, Bled, 2004)
4. EERI. The Tecomán, México Earthquake January 21, 2003, An EERI and SMIS Learning from Earthquakes Reconnaissance Report, Technical Editors S.M. Alcocer and R.E. Klingner, Earthquake Engineering Research Institute, Oakland, California, March 2006
5. A.E. Schultz, *Performance of Masonry Structures During Extreme Lateral Loading Events, Masonry in the Americas* (ACI Publication SP-147, American Concrete Institute, Detroit, 1994), pp. 21–55
6. M. Tomazevic, I. Klemenc, Seismic behaviour of confined masonry walls. *Earthquake Eng. Struct. Dyn.* **26**, 1059–1071 (1997)
7. Suter, G. T., Naguib, E. M. F. (1997). Effect of brick stiffness orthorhropy on the lateral stress in stuck-bonded brick masonry prisms, in *Proceedings, fourth north American masonry conference*, paper 18, 1997
8. P.R. Maiti, A.K. Shukla, Experimental and numerical study to improve lateral load resistance of masonry stack advances in structural engineering and rehabilitation, lecture notes in civil engineering. Springer Nature (2020). https://doi.org/10.1007/978-981-13-7615-3_1
9. P.R. Shukla, A.K. Maiti, Experimental study of confined brick masonry building, advances in structural engineering and rehabilitation, lecture notes in civil engineering. Springer Nature (2020). https://doi.org/10.1007/978-981-13-7615-3_2
10. Page, A.W., Brooks, D.S. Load bearing masonry –review, in *Proceedings of the 7th international brick masonry conference*, pp. 81–99 (1995)
11. Hendry, A.W., Testing methods in masonry engineering, in *Proceedings, fourth north American masonry conference*, 1997
12. ANSYS 2016 User manuals
13. Hilsdorf, H. K. An investigation into the failure mechanism of brick masonry loaded in axial compression. pp. 34–41 (1969)
14. Ali, S., Page, A.W. Finite element model for masonry subjected to concentrated loads, J., *Struct. Division ASCE*, Vol.114, No.8, 1998, pp.1761-1784

Publisher's Note Springer Nature remains neutral with regard to jurisdictional claims in published maps and institutional affiliations.